

# Crystallization and preliminary crystallographic analysis of the signal recognition particle SRP $\Phi$ 14-9 fusion protein

Darcy E.A. Birse<sup>a</sup>, Sylvie Doublé<sup>a,\*\*</sup>, Ulrike Kapp<sup>a</sup>, Katharina Strub<sup>b</sup>, Stephen Cusack<sup>a,\*</sup>, Anders Åberg<sup>a</sup>

<sup>a</sup>European Molecular Biology Laboratory (EMBL), Grenoble Outstation, clo ILL, 156X, 38042 Grenoble Cedex 9, France

<sup>b</sup>Département de Biologie Cellulaire, Université de Genève, Sciences III, CH-1211 Geneva 4, Switzerland

Received 29 February 1996; revised version received 14 March 1996

**Abstract** The SRP $\Phi$ 14-9 fusion protein, which can functionally replace the SRP9/14 heterodimer in the mammalian signal recognition particle (SRP), has been crystallized using the vapor diffusion method. Four different crystal forms were grown. SRP $\Phi$ 14-9 form IV crystals belong to the space group P4<sub>1</sub>22/P4<sub>3</sub>22 with cell parameters  $a = b = 69.7$  Å,  $c = 95.7$  Å,  $\alpha = \beta = \gamma = 90^\circ$ . A complete data set to 2.8 Å resolution with an  $R_{\text{sym}}$  on intensities of 7.0% was collected on a single flash-frozen crystal.

**Key words:** Signal recognition particle (SRP); Fusion protein; Purification; Crystal; X-ray diffraction; Synchrotron

## 1. Introduction

The mammalian signal recognition particle (SRP) is a cytoplasmic ribonucleoprotein particle (RNP) that plays an essential role in the targeting of secretory and membrane proteins to the rough endoplasmic reticulum (RER) (for recent reviews see [1,2]). Targeting occurs co-translationally and translocation across the RER membrane begins before polypeptide synthesis is complete [3–5]. The SRP acts in three distinct ways [6]: it binds the signal sequence of the nascent polypeptide to be translocated [4,6,7], which is exposed on the surface of the translating ribosome [8,9]; it temporarily retards the nascent polypeptide from further elongation [6,10,11]; and it mediates docking of the SRP-ribosome-nascent polypeptide chain complex to the RER membrane via the heterodimeric SRP receptor. With the engagement of this machinery, the SRP is detached and recycled, and co-translational translocation proceeds [12–14].

GTP hydrolysis plays an important role in the SRP cycle, one SRP protein and both subunits of the SRP receptor containing G-domains [2,15]. SRP is not restricted to eukaryotes; SRP-related particles and SRP receptor-related molecules are found ubiquitously and may function in protein translocation in every living organism [16–18].

The mammalian SRP is an 11S cytoplasmic ribonucleoprotein particle which consists of six polypeptides and a single RNA molecule (7S RNA in eukaryotes) [19,20]. The polypeptides are named according to the apparent molecular masses (in kDa) of the canine proteins: SRP9, SRP14, SRP19, SRP54, SRP68, and SRP72. SRP54, which contains a GTP-binding domain, is the signal sequence binding protein and requires SRP19 for efficient binding to SRP RNA. Similarly SRP72 incorporation into SRP requires prior binding of SRP68 to SRP RNA.

In vitro studies show mammalian SRP9 and SRP14 proteins form a tight heterodimer SRP9/14 in the absence of SRP RNA and bind specifically to a region of the SRP RNA which includes both the 3' and 5' ends [21]. The part of SRP comprising SRP9/14 complexed with RNA forms a distinct structural domain known as the *Alu* domain due to the homology of the RNA sequences with the so-called *Alu* family of repetitive DNA sequences and the small cytoplasmic *Alu* RNAs (*scAlus*) [22]. SRP9/14, when bound to the *Alu* region of SRP RNA, forms a stable complex ( $K_d \leq 0.1$  nM) and causes an allosteric change in the SRP RNA conformation [23]. The *Alu* domain of SRP mediates the specific pause(s) or arrest in the synthesis of nascent ER-targeted proteins whose signal sequence has been bound by SRP54 [16]. Both the mechanism and the functional rationale for the elongation arrest activity are unknown although it is hypothesized that the mechanism, before docking with the translocation machinery, prevents translation termination and disengagement from the ribosome.

Primary sequences for several eukaryotic SRP9 and SRP14 proteins have been characterized [24]. No known RNA binding motif has been detected in the sequences. It is possible that SRP9/14 might possess a new RNA binding motif which may be generated upon heterodimerization since neither protein alone binds specifically to SRP RNA. Recently, it has been shown that human SRP9/14 in vivo [7], and SRP14 in vitro [25] can associate as complexes with *scAlu* RNA in so-called *Alu* particles. Furthermore, the human SRP14 is larger than its murine counterpart, this difference being due to a C-terminal alanine/threonine-rich extension [25].

SRP9 can be highly over-expressed in *Escherichia coli* and is stable after purification [26]. SRP9 crystallization is described in the accompanying paper (Doublé et al.). On the other

\*Corresponding author. Fax: (33) 76 20 71 99.  
E-mail: cusack@embl-grenoble.fr

\*\*Present address: Department of Biological Chemistry and Molecular Pharmacology, Harvard Medical School, Boston, MA 02115, USA.

**Abbreviations:** BICINE, *N,N*-bis[2-hydroxyethyl]glycine hydrochloride; CAPS, 3-[cyclohexylamino]-1-propanesulfonic acid; EDTA, *N,N'*-1,2-ethanedithylbis[*N*-(carboxymethyl)glycine]; EMBL, European Molecular Biology Laboratory; ESRF, European Synchrotron Radiation Facility; HEPES, *N*-[2-hydroxyethyl]piperazine-*N'*-[2'-ethanesulfonic acid]; IPTG, isopropyl- $\beta$ -D-thiogalactopyranoside; MES, 2-[*N*-morpholino]ethanesulfonic acid; MPD, 2-methyl-2,4-pentanediol; PAGE, polyacrylamide gel electrophoresis; PEG, polyethylene glycol; PMSF, phenylmethylsulfonyl fluoride; RER, rough endoplasmic reticulum; SDS, sodium dodecyl sulfate; SRP, signal recognition particle; SRP9/14, signal recognition particle proteins SRP9 and SRP14 heterodimer; SRP $\Phi$ 14-9, SRP9/14 fusion protein; TRIS, tris[hydroxymethyl]aminomethane hydrochloride.

hand, expression levels of SRP14 are poor and the protein is unstable. For structural and functional studies a fusion protein, denoted SRPΦ14-9, has been constructed which mimics the SRP9/14 heterodimer [26]. SRPΦ14-9 is a single polypeptide over-expressed in *Escherichia coli*, which can be purified to homogeneity and which is significantly more stable than the SRP9 and SRP14 proteins alone. The SRPΦ14-9 gene contains in its 5' region a sequence coding for the peptide MASMTGGQMGRIPGNSPR (a cloning remnant) followed by the complete coding sequence of the mouse SRP14 (110 amino acid residues and has a molecular weight of 12.5 kDa) followed by a linker sequence of 51 base pairs and the complete coding sequence of the mouse SRP9 (86 amino acid residues and has a molecular weight of 10.2 kDa). The linker sequence encodes 17 amino acids that contain the well characterized epitope (–EQKLISEED) for the monoclonal antibody against the human Myc protein. The complete SRPΦ14-9 fusion protein contains 232 amino acid residues and has a molecular weight of 26.7 kDa.

SRPΦ14-9 can functionally replace the SRP9/14 heterodimeric subunit in the SRP. It binds SRP RNA and functions in elongation arrest and release of elongation arrest without loss of activity compared to the native SRP9/14 heterodimer [26]. Two constructions of the fusion protein SRPΦ14-9 and SRPΦ9-14, differing in the order of arrangement of SRP9 and SRP14 in the polypeptide, have been shown to be equally active, indicating that the free N- or C-termini in either protein, SRP9 or SRP14, are not essential structural elements in the function of the SRP9/14 heterodimer in the SRP. The over-expressed SRPΦ14-9 greatly facilitates the structural and functional analysis of SRP9, SRP14, heterodimer SRP9/14 and their interactions with SRP RNA.

In this and the accompanying paper we describe the crystallization of SRPΦ14-9 and SRP9, this being the first report of crystals of components of the mammalian SRP. Whereas many functional and biological aspects of SRP are understood, detailed structural information is completely lacking. The crystal structure of SRPΦ14-9 will provide information about protein/protein and protein/RNA interactions as well as being the first step to understand the structural basis of the SRP *Alu* domain mediated elongation arrest.

## 2. Materials and methods

### 2.1. Expression and purification of the SRPΦ14-9 fusion protein

Mouse SRPΦ14-9 fusion protein was cloned in pET3c expression vector and over-expressed in *Escherichia coli* BL21/lysS [26].

Bacteria were grown in LB medium containing 50 µg/ml of ampicillin in an 18 liter fermenter at 37°C. SRPΦ14-9 protein synthesis was induced with 0.8 mM isopropyl-β-D-thiogalactopyranoside (IPTG) at

OD<sub>600</sub> ≈ 0.6 for 3 h. The cells were harvested by centrifugation and frozen in aliquots at –80°C. 5 g of cells were suspended in 15 ml of 50 mM TRIS-HCl pH 7.5, 10 mM MgCl<sub>2</sub>, 10 mM β-mercaptoethanol, 10% glycerol, 1.0 mg of DNase, 500 µM Pefabloc and the NaCl concentration was adjusted to 250 mM. Cells were lysed in a French press (1000 psi) after which 10 mM EDTA was added. The lysate was clarified by centrifugation at 4°C for 20 min at 15 000 × g. 0.2% Polymyxin P was added to the supernatant, incubated on ice for 15 min, then centrifuged at 4°C for 15 min at 12 000 × g.

The supernatant was loaded on a heparin column (two sequential Bio-Rad 5 ml columns) equilibrated with buffer A (250 mM NaCl, 10 mM Tris-HCl pH 7.5, 10 mM β-mercaptoethanol and 1.0 mM EDTA). SRPΦ14-9 protein was eluted with a 60 ml gradient from buffer A to buffer B (1.0 M NaCl, 10 mM Tris-HCl pH 7.5, 10 mM β-mercaptoethanol and 1.0 mM EDTA). SRPΦ14-9 protein containing fractions were collected and precipitated with 70% saturated ammonium sulfate, incubated for 4 h on ice, then centrifuged at 15 000 × g for 20 min.

The protein pellet was dissolved in 200 mM NaCl, 50 mM sodium phosphate pH 7.5, 10 mM β-mercaptoethanol, 1.0 mM EDTA and 500 µM phenylmethylsulfonyl fluoride (PMSF) then dialyzed against the same buffer overnight at 4°C. The protein was loaded on a Mono-S HR5/5 column (Pharmacia-FPLC system) equilibrated with buffer C (200 mM NaCl, 50 mM Na/K PO<sub>4</sub> pH 7.5). SRPΦ14-9 protein was eluted with a 20 ml linear NaCl gradient from buffer C to buffer D (500 mM NaCl, 50 mM Na/K PO<sub>4</sub> pH 7.5) and precipitated with 70% saturated ammonium sulfate as mentioned above.

Pure SRPΦ14-9 protein was dialyzed against 500 mM (NH<sub>4</sub>)<sub>2</sub>SO<sub>4</sub>, 10 mM Tris-HCl pH 8.0 or against 500 mM Na/K PO<sub>4</sub> pH 7.5 at 4°C then concentrated to 10 mg/ml using Centricon-10 concentrators.

### 2.2. Crystallization procedures

Initial crystallization conditions were obtained using incomplete factorial designs [27] and optimized using response surface experiments [28,29]. The crystallization conditions utilized various precipitants such as sulfates, phosphates, polyethylene glycols (PEGs) and 2-methyl-2,4-pentanediol (MPD), with concentrations ranging from 300 mM to 2.9 M; various buffers such as acetate, citrate, MES, cacodylate, BICINE, HEPES, Tris, borate and CAPS, in their respective pH ranges from pH 4.0 to pH 11.0, in the concentration range from 20 mM to 200 mM; a wide range of salts such as ammonium, calcium, lithium, magnesium, manganese, potassium and sodium in the concentration range from 500 µM to 50 mM; and a number of additives or detergents such as n-octyl-β-D-glucopyranoside, dimethyl sulfoxide, glycerol, isopropyl alcohol, Nikkol and MPD, in the percentage range of 0.1% to 10%.

The crystallization trials applied the hanging drop vapor diffusion method on silicized glass cover slides in Linbro plates. Drops contained 2 µl of protein solution at 5–10 mg/ml and were mixed with equal volumes of reservoir solution and allowed to equilibrate against 1.0 ml of reservoir solution at 4°C or 22°C.

## 3. Results and discussion

Crystallization conditions were found using an incomplete factorial design [27]. A crystallization data base [30] was searched for conditions used for ribosomal proteins, which are also small, basic, RNA binding proteins. The data base

Table 1  
Native SRPΦ14-9 data<sup>a</sup>

	30.0–2.80 Å resolution	2.95–2.80 Å resolution shell
Number of observations ( $I/\sigma I > 1$ )	31 918	4 293
Number of unique observations	5 798	755
Average $I/\sigma I$	6.4	2.7
Completeness	94.5%	94.4%
Percentage $I/\sigma I > 3$	86.0%	67.1%
Multiplicity	5.5	5.3
$R_{\text{sym}}[\sum  I_i - \langle I \rangle  / \sum I_i]$	7.0%	28.0%

<sup>a</sup>Data were collected at the MAD Beamline: BL19 (D-14) at the ESRF using 0.927 Å radiation. Data were collected on a single flash-frozen crystal at 100 K with a crystal-to-film distance of 420 mm on a 30 cm Mar Research image plate. Forty-two contiguous 1.5° oscillation rotation images were collected to 2.8 Å resolution followed by 22 2.0° oscillation rotation images collected to 4.0 Å resolution.

search showed that the ribosomal proteins in the data bank had been crystallized using sodium potassium phosphate, ammonium sulfate, or MPD, at a pH ranging from 7.2 to 8.5. The initial incomplete factorial experiments gave rise to two crystal forms: crystal form I grown in ammonium sulfate and PEG at pH 6.5, and crystal form III, grown using sodium potassium phosphate at pH 7.5, and MPD as an additive.

The crystal form I of SRP $\Phi$ 14-9 was grown mixing high molecular weight PEG and ammonium sulfate as precipitants in hanging drop vapor diffusion experiments at room temperature. This precipitant mixture formed a solvent front where nucleation took place and sustained crystal growth occurred. During crystal growth, the crystals descended from the solvent front to a resting position at the bottom of the drop where further growth occurred. The reservoirs contain 28–32% PEG 8000, 200 mM (NH<sub>4</sub>)<sub>2</sub>SO<sub>4</sub>, 100 mM MES-KOH pH 6.5, 1.0 mM NaN<sub>3</sub> and 100  $\mu$ M PMSF. Addition of dithiothreitol (DTT) was found to prevent crystallization. These crystals were difficult to reproduce and difficult to manipulate. When harvesting crystals, difficulties ensued when the cover slide was inverted. The equilibrated drop went from a solvent front stable state to a turbulent, whirlpool-like environment of mixing solutions causing the crystal to be spun about the drop, rapidly dissolving or damaging the crystal. Applying other methods, such as sitting drop or capillary crystallization techniques, resulted in poor quality crystals or no observed crystal nucleation.

A second crystallization condition (crystal form II) grew in 30–34% saturated ammonium sulfate, 50 mM MES-KOH pH 6.0 and 1.0 mM NaN<sub>3</sub>, at room temperature. These crystals were not consistently reproducible and were difficult to manage due to crystal size and fragility. No data has been collected on these crystals.

For form I and form II SRP $\Phi$ 14-9 protein crystals, the average crystal dimensions were  $50 \times 50 \times 30 \mu\text{m}^3$  and crystals appeared after approximately 1 month. Form I crystals belong to the tetragonal space group  $I4_1$  with unit cell parameters  $a = b = 128.6 \text{ \AA}$ ,  $c = 172.1 \text{ \AA}$ ,  $\alpha = \beta = \gamma = 90^\circ$  and a unit cell volume of  $2.83 \times 10^6 \text{ \AA}^3$ . The unit cell volume is consistent with the presence of 4 molecules per asymmetric unit corresponding to a specific volume  $V_m = 3.48 \text{ \AA}^3/\text{Da}$  and solvent content of 65% [31]. X-ray diffraction experiments



Fig. 1. Photograph of bipyramidal SRP $\Phi$ 14-9 crystals. Typical drop showing SRP $\Phi$ 14-9 protein crystals with average dimensions  $150 \times 150 \times 300 \mu\text{m}^3$  with single (NH<sub>4</sub>)<sub>2</sub>HPO<sub>4</sub> salt crystal in background.

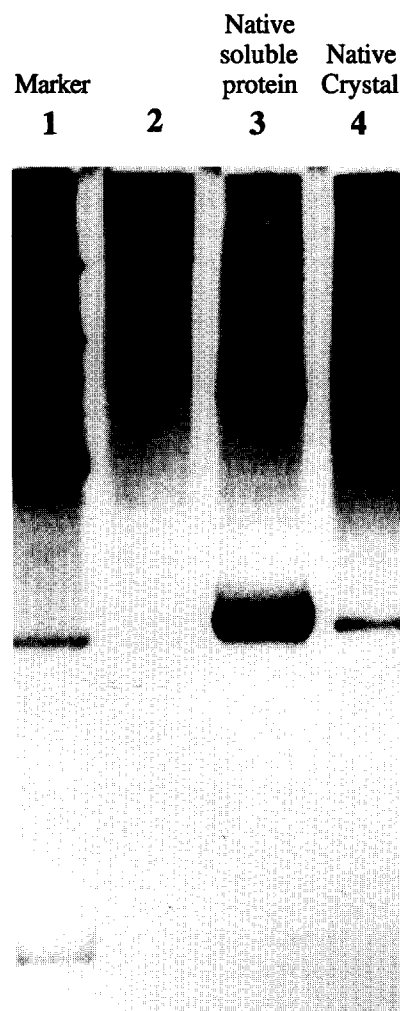


Fig. 2. Photograph of a silver stained PAGE-SDS gel, showing SRP $\Phi$ 14-9 washed and dissolved crystals (lane 4) and native soluble SRP $\Phi$ 14-9 protein (lane 3). The bands migrate equally in gel indicating no degradation of SRP $\Phi$ 14-9 into SRP9 or SRP14.

on these crystals showed diffraction beyond  $3.2 \text{ \AA}$  resolution. Crystals were extremely X-ray sensitive and suffered severe radiation damage after several exposures. Due to this constraint, effective cryoprotectants for cryogenic experiments (100 K) were screened. A buffered solution of 30% glycerol mixed with 30% saturated ammonium sulfate acted as an effective cryoprotectant. An 80% complete data set to a resolution of  $4.0 \text{ \AA}$  with an  $R_{\text{sym}}$  on intensities of 7.2% was collected from a single flash-frozen crystal (100 K) on a MAR Research image plate at the ESRF-Beamline 19 (D-14).

Due to the problems of crystal reproducibility, size and handling, other crystallization conditions were sought. The initial incomplete factorial experiment revealed that SRP $\Phi$ 14-9 can be crystallized with the morphology of small rectangular plates (crystal form III) using sodium potassium phosphate as a precipitant. The crystals diffracted beyond  $3.3 \text{ \AA}$  resolution but were not reproducible. Further precipitant gradients were used to screen for a reproducible crystallization condition using various phosphate mixtures. Mixtures of disodium hydrogen/monosodium dihydrogen/dipotassium hydrogen/monopotassium dihydrogen phosphates were used as both precipitants and buffers. This phosphate mixture combined

with 2% MPD and 1.0 mM  $\text{NaN}_3$  yielded square-base pyramidal or bipyramidal crystals (crystal form IV) after 10–12 days with typical dimensions of  $150 \times 150 \times 300 \mu\text{m}^3$ .

The conditions for growing form IV crystals consist of a reservoir of 1.6–2.2 M  $\text{Na}_2\text{H}/\text{NaH}_2/\text{K}_2\text{H}/\text{KH}_2\text{PO}_4$  mixture at pH 7.5, 2% MPD and 1.0 mM  $\text{NaN}_3$  at 4°C. The protein solution contains 500 mM  $(\text{NH}_4)_2\text{SO}_4$  and 10 mM Tris-HCl pH 8.0. The ammonium sulfate is necessary to keep the protein soluble. As expected, upon mixing with the reservoir solution,  $(\text{NH}_4)_2\text{HPO}_4$  crystals are formed, altering both the soluble sulfate and soluble phosphate concentrations in the drop. Formation of form IV crystals is preceded by growth of a large  $(\text{NH}_4)_2\text{HPO}_4$  crystal, followed shortly by the nucleation and growth of SRPΦ14-9 protein crystals (Fig. 1). This procedure is reproducible.

A native SRPΦ14-9 crystal taken from its mother liquor in a hanging drop was washed and dissolved then run on a PAGE-SDS gel alongside soluble protein (Fig. 2). The silver stained gel shows that all three samples migrate equally as single bands, indicating no degradation into SRP9 or SRP14 proteins.

Changes in pH alter the morphology of the crystals such that at pH 5.0 they grow as elongated pyramids, whereas at pH 7.5 they are bipyramidal. A suitable cryoprotectant for these crystals consists of 2.3–2.7 M  $\text{Na}_2\text{H}/\text{NaH}_2/\text{K}_2\text{H}/\text{KH}_2\text{PO}_4$  mixture at pH 7.5 and 20–30% MPD.

X-ray diffraction experiments on flash-frozen crystals in a cold stream of nitrogen at 100 K showed diffraction beyond 2.3 Å resolution. The crystals belong to the tetragonal space group  $\text{P4}_122/\text{P4}_322$  with cell parameters  $a = b = 69.7$  Å,  $c = 90.7$  Å,  $\alpha = \beta = \gamma = 90^\circ$  and a unit cell volume of  $4.65 \times 10^5$  Å<sup>3</sup>. This is consistent with one molecule of SRPΦ14-9 per asymmetric unit,  $V_m = 2.28$  Å<sup>3</sup>/Da and solvent content of 46%.

A complete native data set to a resolution of 2.8 Å was collected on a single flash-frozen crystal on a Mar Research image plate detector at the ESRF-Beamline 19 (D-14). Images were collected with an oscillation range of  $1.5^\circ$  for a data set to 2.8 Å resolution and of  $2.0^\circ$  oscillations for a low resolution data set to 4.0 Å. The images were auto-indexed and intensities integrated using DENZO [32]. Data were scaled and merged using the CCP4 program package [33]. The overall  $R_{\text{sym}}$  of intensities was 7.0%, with a redundancy of 5.5 to 2.8 Å (Table 1).

Selenomethionyl SRPΦ14-9 has been overexpressed, purified and crystallized and will be used as a derivative in order to solve the phase problem either by multiple isomorphous replacement (MIR) or multiwavelength anomalous diffraction (MAD) methods.

**Acknowledgements:** The authors wish to thank Andy Thompson (EMBL) for help on the MAD Beamline: BL 19 (D-14) and Bjarne

Rasmussen (EMBL) for help on High Brilliance Beamline: BL 4 (ID-2) at the European Synchrotron Radiation Facility (ESRF), Grenoble, France. We also wish to thank Dr. Elizabeth DiCapua who was involved at an early stage in this project.

## References

- [1] Walter, P. and Johnson, A.E. (1994) *Annu. Rev. Cell Biol.* 10, 87–119.
- [2] Lütcke, H. (1995) *Eur. J. Biochem.* 228, 531–550.
- [3] Prehn, S., Wiedmann, M., Rapoport, T.A. and Zwieb, C. (1987) *EMBO J.* 6, 2093–2097.
- [4] Campos, N., Palau, J., Torrent, M. and Ludevid, D. (1988) *J. Biol. Chem.* 263, 9646–9650.
- [5] Hann, B.C. and Walter, P. (1991) *Cell* 67, 131–144.
- [6] Siegel, V. and Walter, P. (1988) *Cell* 52, 39–49.
- [7] Chang, D.-Y., Nelson, B., Bilyeu, T., Hsu, K., Darlington, G.J. and Maraia, R.J. (1994) *Mol. Cell. Biol.* 14, 3949–3959.
- [8] Wiedmann, M., Kurzchalia, T.V., Bielka, H. and Rapoport, T.A. (1987) *J. Cell. Biol.* 104, 201–208.
- [9] Crowley, K.S., Reinhart, G.D. and Johnson, A.E. (1993) *Cell* 73, 1101–1115.
- [10] Wolin, S. and Walter, P. (1988) *EMBO J.* 7, 3559–3569.
- [11] Wolin, S.L. and Walter, P. (1989) *J. Cell. Biol.* 109, 2617–2622.
- [12] Connolly, T. and Gilmore, R. (1989) *Cell* 57, 599–610.
- [13] Connolly, T., Rapiejko, P.J. and Gilmore, R. (1991) *Science* 252, 1171–1173.
- [14] Görlich, D., Hartmann, E., Prehn, S. and Rapoport, T.A. (1992) *Nature* 357, 47–52.
- [15] High, S. (1995) *Prog. Biophys. Mol. Biol.* 63, 233–250.
- [16] Ribes, V., Römisch, K., Giner, A., Dobberstein, B. and Tollervey, D. (1990) *Cell* 63, 591–600.
- [17] Nakamura, K., Imai, Y., Nakamura, A. and Yamane, K. (1992) *J. Bacteriol.* 174, 2185–2192.
- [18] Lührink, J., ten Hagen-Jongman, C.M., v.d. Weijden, C.C., Oudega, B., High, S., Dobberstein, B. and Kusters, R. (1994) *EMBO J.* 13, 2289–2296.
- [19] Walter, P. and Blobel, G. (1980) *Proc. Natl. Acad. Sci. USA* 77, 7112–7116.
- [20] Walter, P. and Blobel, G. (1982) *Nature* 299, 691–698.
- [21] Strub, K., Moss, J. and Walter, P. (1991) 11, 3949–3959.
- [22] Wiener, A.M. (1980) *Cell* 22, 209–218.
- [23] Janiak, F., Walter, P. and Johnson, A.E. (1992) *Biochemistry* 31, 5830–5840.
- [24] Larsen, N. and Zwieb, C. (1996) *Nucleic Acids Res.* 24, 80–81.
- [25] Bovia, F., Fornallaz, M., Leffers, H. and Strub, K. (1995) *Mol. Cell. Biol.* 6, 471–484.
- [26] Bovia, F., Bui, N. and Strub, K. (1994) *Nucleic Acids Res.* 22, 2028–2035.
- [27] Carter Jr., C.W. and Carter, C.W. (1979) *J. Biol. Chem.* 254, 12219–12223.
- [28] Carter Jr., C.W. and Yin, Y. (1994) *Acta Cryst. D50*, 572–590.
- [29] Carter Jr., C.W., Doublie, S. and Coleman, D.E. (1994) *J. Mol. Biol.* 238, 346–365.
- [30] Gilliland, G.L., Tung, M., Blakeslee, D.M. and Ladner, J. (1994) *Acta Cryst. D50*, 408–413.
- [31] Matthews, B.W. (1968) *J. Mol. Biol.* 33, 491–497.
- [32] Otwinowski, Z., DENZO. A Film Processing Program for Macromolecular Crystallography. Yale University, New Haven, CT, 1991.
- [33] CCP4 (1994) *Acta. Cryst. D50*, 760–763.